NOP3 Is an Essential Yeast Protein Which Is Required for Pre-rRNA Processing

Iain D. Russell and David Tollervey

European Molecular Biology Laboratory, D-6900 Heidelberg, Germany

Abstract. The four nucleolar proteins NOP1, SSB1, GAR1, and NSR1 of *Saccharomyces cerevisiae* share a repetitive domain composed of repeat units rich in glycine and arginine (GAR domain). We have cloned and sequenced a fifth member of this family, *NOP3*, and shown it to be essential for cell viability. The *NOP3* open reading frame encodes a 415 amino acid protein with a predicted molecular mass of 45 kD, containing a GAR domain and an RNA recognition motif. NOP3-specific antibodies recognize a 60-kD protein by SDS-PAGE and decorate the nucleolus and the surrounding nucleoplasm. A conditional lethal mutation, *GAL::nop3*, was constructed; growth of the mutant strain in glucose medium represses *NOP3* expression. In cells depleted of NOP3, production of cytoplasmic ribosomes is impaired. Northern analysis and pulse–chase labeling indicate that pre-rRNA processing is inhibited at the late steps, in which 27SB pre-rRNA is cleaved to 25S rRNA and 20S pre-rRNA to 18S rRNA.

THE eukaryotic nucleolus is the site of transcription of preribosomal RNA (pre-rRNA)[1] by RNA polymerase I and its subsequent processing and assembly with ribosomal proteins to form ribosomal particles, and is therefore essential for ribosome biogenesis. In the budding yeast, *Saccharomyces cerevisiae*, the nucleolus has been described as the "dense crescent" filling ~30% of the nucleus. To support the diverse functions of the nucleolus, a large number of accessory factors known to include both RNA and protein must be present to allow transcription, modification, and processing of the rRNA and transport of all the necessary components (for a recent review, see Hernandez-Verdun, 1991).

It has been known for some time that a large number of small nucleolar RNAs (snoRNAs) are associated with the pre-rRNA (Tollervey, 1987; Zagorski et al., 1988) and at least the U3 (Hughes and Ares, 1991), U14 (Li et al., 1990), snR10 (Tollervey, 1987), and snR30 (Morrissey, J. P., and D. Tollervey, manuscript submitted for publication) snoRNAs are required for cleavage of the pre-rRNA transcript to yield mature rRNA. By analogy to the small nuclear RNAs (snRNAs) involved in mRNA splicing, a large number of protein components are expected to be associated with the various snoRNAs. Previous studies have identified a large number of nucleolar proteins involved in rRNA transcription and its regulation, but only a few factors required for pre-rRNA processing or ribosome assembly have been characterized. These include GAR1 (Girard et al., 1992), NOP1 (Schimmang et al., 1989; Henríquez et al., 1990), NSR1 (Lee et al., 1991), and SSB1 (Jong et al., 1987) in yeast and fibrillarin (Ochs et al., 1985) and nucleolin (Lapeyre et al., 1987) in vertebrates. All of these proteins share a conserved repetitive domain rich in glycine and arginine known as the GAR domain and appear to represent a nucleolar protein family. Yeast GAR1, NOP1, and SSB1 (Clark et al., 1990; Tollervey et al., 1991; Girard et al., 1992) and human fibrillarin (Tyc and Steitz, 1989) have been shown to be associated with the snoRNAs.

Sequence comparison suggests that the secondary or tertiary structure of the GAR domain, rather than the primary sequence, has been conserved in evolution. The GAR domain consists of repeating units of RGGFRGG or RGGFGGR (where F can be substituted by either S, Y, or A); however, degenerate spacing and sequence between repeats appears to be tolerated. The domain is structurally separated from the remainder of the protein by flanking proline residues (Girard et al., 1992), which are predicted to prevent structural continuity with adjacent domains because of their helix destabilizing properties. Perhaps because of this, the GAR domain appears to be able to function independently of its location within the protein. GAR domains are located in the central region of SSB1, at the NH_2 terminus of NOP1, at the COOH terminus of nucleolin, and at both termini of GAR1.

Recently, Ghisolfi et al. (1992) showed that the isolated GAR domain of vertebrate nucleolin adopts a repeated β-turn structure capable of binding single-stranded nucleic acid and destabilizing RNA helices. It is proposed that the binding affinity of nucleolin, which contains four RNA recognition motifs, is increased by the presence of the GAR domain, which binds RNA substrates nonspecifically.

To isolate further nucleolar proteins involved in pre-rRNA

1. *Abbreviations used in this paper:* GAR domain, a conserved repetitive domain rich in glycine and arginine; MNB, mini-nucleolar bodies; PCR, polymerase chain reaction; pre-rRNA, preribosomal RNA; snoRNA, small nucleolar RNA; snRNA, small nuclear RNA.

maturation, we have screened an *S. cerevisiae* library for proteins of the glycine/arginine repeat family. Using the region of NOP1 encoding the glycine/arginine repeat as a hybridization probe, we show that this family includes at least six members. With this approach we isolated clones encoding SSB1 and NSR1 in addition to a novel protein that we have called NOP3.

We report here the sequence of NOP3, a protein containing a single glycine/arginine repeat domain located at its carboxy terminus. NOP3 is localized in the nucleus and plays a role in the maturation of pre-rRNA.

Materials and Methods

Strains and Media

Growth and handling of *S. cerevisiae* involved standard techniques. YPD media contained yeast extract 1%, peptone 2%, and glucose 2%. Transformation was by the lithium acetate method of Ito et al. (1983). The diploid strain used for the gene disruption experiments carries *MATa, ade8, his4, his3, ade2, leu2-3, 112, lys1, ura3-52*; *MATα, ade2, leu2, lys1*, and *ura3* (strains JU4.2 × JR26.19B; kindly provided by E. Hurt, EMBL, Heidelberg). The *NOP3*$^+$ haploid strain carries *MATa, ura3-52, leu2-3,112, ade1-100, his4-519*, and is GAL$^+$ (strain BWG1-7A; kindly provided by L. Guarente, Cambridge, Massachusetts); the strain used for NOP3 depletion is isogenic except that it was transformed with the *URA3-GAL::nop3* construct that was integrated at the *NOP3* chromosomal locus. The RNA polymerase I-deficient strain used for immunofluorescence carries *MATα, rpa135::LEU2, ade2-1, ura3-1, his3-11, trp1-1, leu2-3,112*, and *can1-100*, pNOY102 (strain NOY408-1a; Nogi et al., 1991).

For NOP3 depletion, cells growing exponentially in galactose minimal medium were harvested by centrifugation, washed, and resuspended in glucose minimal medium. During growth, cells were diluted in prewarmed medium to maintain growth in the early exponential phase. The growth curve was drawn using the Cricket Graph program.

Southern Blot Analysis

Total yeast genomic DNA was extracted according to Dandekar and Tollervey (1989). DNA was digested (KpnI, BamHI, HindIII, BglII, ClaI, EcoRI, and SalI), electrophoresed on a 0.8% agarose gel, and transferred and cross-linked to Hybond-N (Amersham International plc, Amersham, UK) as described in Maniatis et al. (1989). Filters were prehybridized 1 h at 37°C in 5× SSPE (Maniatis et al., 1989), 40% formamide, 5× Denhardt's, 1% SDS, and 4 mg/ml hearing sperm DNA. The GAR riboprobe was added directly to this buffer and filters were hybridized for 12 h at 37°C. Filters were washed twice in 1× SSPE at 37°C and once in 0.1× SSPE/0.1% SDS at 50°C before autoradiography at −70°C for 12 h with an intensifying screen.

Isolation of the Genomic NOP3 Clone

An *S. cerevisiae Sau3A* partial genomic library constructed in YEp24 was kindly provided by M. Carlson. Colony hybridization was performed as described in Maniatis et al., (1989) using the same conditions described for the genomic Southern hybridization. Approximately three genomic equivalents were screened.

Raising and Purification of Antibodies against NOP3

Rabbit polyclonal antibodies were generated against the peptide [NH_2]-KYRTRDAPRERSPTR-[COOH] corresponding to the 14 carboxy-terminal proximal residues. A lysine residue was included at the amino terminus of the peptide to facilitate covalent cross-linking by glutaraldehyde to the carrier protein, keyhole limpet haemocyanin (Calbiochem Corp., La Jolla, CA).

Antibodies used in the immunofluorescence studies were affinity-purified against the peptide immobilized on Sepharose beads. 1.5 ml of serum was incubated with Sepharose-peptide beads for 12 h at 4°C. The beads were washed with 20 ml of PBS in a column. Antibodies were eluted from the column with 3 ml of glycine, pH 2.2. Each 500-μl fraction collected was neutralized with 10 μl of 1.5 M Tris, pH 8.8. The antibody concentration in each fraction was determined by measuring OD_{280}.

Immunofluorescence

Tetraploid cells were grown in YPD and harvested in exponential phase by centrifugation at 4°C, washed, and incubated 10 min in 0.1 M Tris-HCl/10 mM DTT. The cells were spheroplasted for 10 min at 30°C in spheroplast buffer (1.2 M sorbitol/20 mM $KHPO_4$, pH 7.4). The cells were washed once in spheroplast buffer before a 1.5-h incubation at 30°C in recovery buffer (2.4 M sorbitol diluted 1:1 in YPD). Cells were fixed by adding an equal volume of 8% paraformaldehyde and incubating 10 min at room temperature. The cells were harvested, washed twice with PBS, and applied to glass coverslips precoated with poly-L-lysine. Cells were stained as described by Tollervey et al. (1991). Primary antibodies were monoclonal anti-NOP1 (mAb A66) (Henríquez et al., 1990; generously provided by J. P. Aris, Rockefeller University, New York) and affinity-purified anti-NOP3 (C4-1.2), followed by second antibodies, FITC goat anti-mouse and Texas Red goat anti-rabbit IgGs (Jackson Immunoresearch Laboratories, Inc., West Grove, PA).

The compact confocal microscope used in the study was developed and built at the EMBL (Heidelberg, Germany). An excitation wavelength of 488 nm (FITC) and 529 nm (Texas Red) was selected from an argon-ion laser. Pseudo-colored images of both signals were generated and superimposed. Images were photographed on Fujichrome 100 film using a Polaroid Freeze Frame Recorder.

Construction of the nop3::URA and GAL::nop3 Strains

Polymerase chain reaction (PCR) primers were used to amplify a 262-bp and an 800-bp fragment corresponding to the 5′ and 3′ untranslated regions of *NOP3*, respectively. A complementary overlap between primers allowed the complete 5′ and 3′ regions of *NOP3* to be amplified in a second round of PCR. The primers were designed with convenient restriction sites to subclone a HindIII-BamHI *URA3-pGAL10* fragment excised from the plasmid, pLGSD5 (Guarente et al., 1982). The *GAL::nop3* strain was constructed in a similar manner; the same 5′ region was amplified, but different primers were used to amplify a 321-bp internal *NOP3* fragment including the ATG. After a second round PCR reaction, the HindIII-BamHI *URA3-pGAL10* fragment from pLGSD5 was subcloned, resulting in the construct 5′ *NOP3* flanking sequence *URA3-pGAL10*-ATG-*NOP3* coding sequence. In each case transformation selecting for *URA3*$^+$ resulted in the exact replacement of *NOP3* by the corresponding construct at the *NOP3* locus in the chromosome.

Pulse Labeling of Protein and RNA

Proteins and RNA were pulse labeled in vivo as described by Tollervey et al. (1991). Incorporation of radioactivity was measured before separation of ribosomal subunits. Comparable amounts of radioactivity for the *GAL::nop3* and the *NOP3*$^+$ strains were subjected to sucrose gradient centrifugation.

Northern Hybridization

RNA extraction, polyacrylamide and agarose-formaldehyde gel electrophoresis, and hybridization were performed as described by Tollervey et al. (1991).

Pulse-Chase Labeling of RNA

Pulse-chase labeling, RNA extraction, agarose-formaldehyde gels, and fluorography was performed as described by Tollervey et al. (1991).

Results

Identification and Cloning of GAR Proteins

To investigate the extent of the GAR protein family in *S. cerevisiae*, the region that encodes the amino terminus of *NOP1* (Schimmang et al., 1989) was used as a hybridization probe (GAR riboprobe) at reduced stringency against an *S. cerevisiae* genomic Southern hybridization. The GAR riboprobe was transcribed using T7 RNA polymerase from the pBluescript vector (Stratagene Inc., La Jolla, CA) terminat-

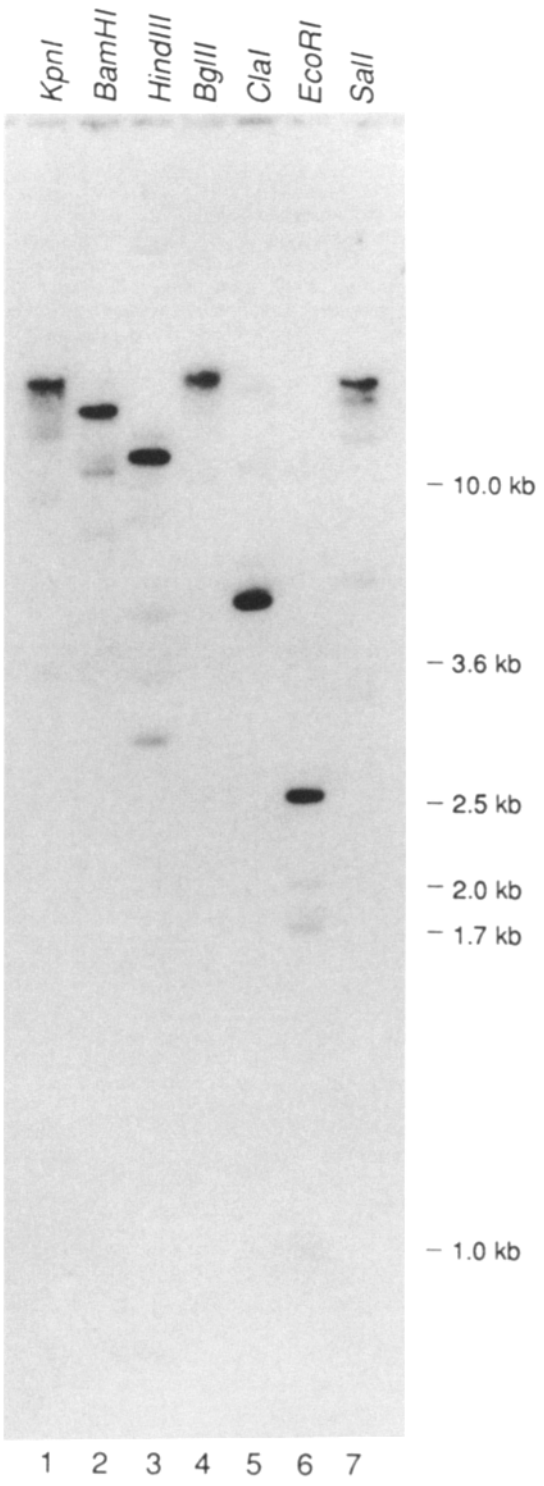

Figure 1. Southern analysis of yeast genomic DNA with GAR riboprobe. 5 μg of total yeast genomic DNA was digested with various restriction enzymes and separated by electrophoresis on a 0.8% agarose gel before transfer to Hybond-N. The filter was hybridized at reduced stringency with the GAR riboprobe. Six cross-hybridizing species are present in each lane, the strong band in each case corresponding to *NOP1*. The estimated sizes of the EcoRI fragments are shown at the right.

ing at the *StyI* site 2 nucleotides 3′ to the GAR domain of *NOP1*, and contained an additional 22 nucleotides of upstream *NOP1* sequence. In addition to *NOP1*, the probe identified five cross-hybridizing species in genomic DNA digested with a number of different restriction enzymes (see Fig. 1).

To clone the cross-hybridizing genes, the GAR riboprobe was used to screen an *S. cerevisiae* genomic library at reduced stringency. From approximately three genomic equivalents screened, 41 positive clones were identified and carried through for further analysis. Restriction mapping and Southern analysis showed these to represent four distinct loci (excluding NOP1 itself). Sequence analysis showed these to encode two previously identified GAR proteins, SSB1 (Jong et al., 1987) and NRS1 (Lee et al., 1991), and one previously unidentified protein that we designate NOP3. The sequence obtained for the *SSB1* clone differed slightly from the published sequence (Jong et al., 1987). Our sequence shows an additional G at position +484, resulting in the insertion of one amino acid residue and the substitution of 19 amino acids; two additional A bases are inserted at positions +520 and +540, restoring the original reading frame. These discrepancies may be due to strain differences. The revised sequence has been submitted to the EMBL data library, accession number X66278.

NOP3 Encodes a 45-kD Protein That Is Essential for Viability

A 6-kb SalI fragment was subcloned and restriction mapped (Fig. 2 *A*). The *NOP3* open reading frame is 1,245 bp in length and encodes a protein of 415 amino acid residues with a predicted molecular mass of 45 kD. A single product, presumably representing the transcription start site, was detected by primer extension analysis at position −23 relative to the ATG (data not shown). A putative TATA box lies 33 bases upstream from this position at −56 relative to the ATG. *NOP3* contains a single GAR domain spanning ~100 amino acids located at the carboxy terminus of the protein (Fig. 2 *B*). This is the only region of homology with NOP1, showing 72% similarity (62% identity) over 105 amino acids to the GAR domain of *NOP1*. Using the FASTA program to search the EMBL/GenBank database, the *NOP3* sequence recognized all the known GAR proteins as the highest matches. In each case the similarity was restricted to the GAR domain. The amino-terminal region of *NOP3* shows a proline-glutamic acid dimer repeated every three to four residues over a 30-residue stretch. An RNA recognition motif matching the consensus (reviewed by Kenan et al., 1991) is present in the central region of *NOP3*; the highly conserved RNP1 sequence is located at +472 in the DNA sequence (Fig. 2 *B*).

A PCR approach was used to perform a gene disruption experiment in which the complete open reading frame for *NOP3* was replaced by the *URA3* marker gene. The *nop3::URA3* construct was inserted at the chromosomal locus by homologous recombination and correct integration at the *NOP3* locus was verified by Southern analysis of chromosomal DNA from the diploid (Fig. 3 *A*). Two EcoRI fragments of 1 and 1.85 kb are detected in the nontransformed strain (Fig. 3 *A*, lane *1*) due to the presence of an EcoRI site within the *NOP3* coding sequence. An additional 2.4-kb

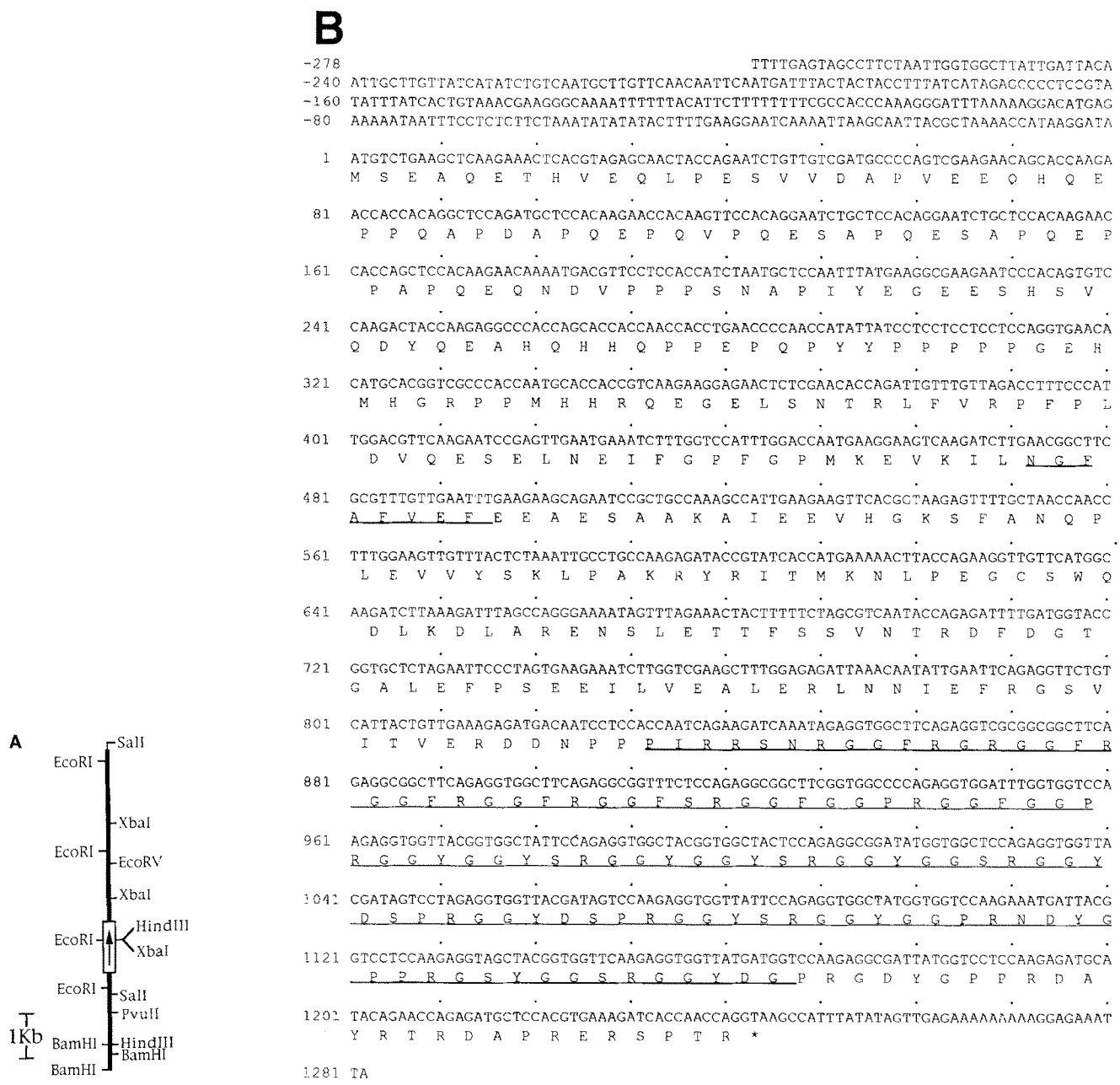

Figure 2. NOP3 encodes a 415 amino acid polypeptide. (*A*) Restriction map of the *NOP3* gene within the chromosomal fragment contained in YEp24. *NOP3* is centrally located within the 6.3-kb insert and the direction of transcription is indicated by the arrow. The leftmost SalI site is located within the YEp24 vector sequence, represented by the narrow section of the line. (*B*) Primary sequence of the *NOP3* gene and the corresponding amino acid sequence which is given below. Position number 1 corresponds to the initiation codon. The GAR domain, located at +832 to +1,167, and the highly conserved RNP1 sequence of the RRM, located at +472 to +495, are underlined. A putative TATA box lies at −56 relative to the ATG and the presumed transcription start site was mapped at position −23 relative to the ATG by primer extension analysis. The *NOP3* open reading frame is 1,245 bp, encoding a 415 amino acid protein. These sequence data are available from EMBL/GenBank/DDBJ under accession number X66019.

fragment is detected in the transformed strains (Fig. 3 *A*, lanes *2* and *3*), consistent with the replacement of *NOP3* by *nop3::URA3*. After sporulation, the transformed diploid yielded only two viable spores from each tetrad, confirming that *NOP3* is essential for cell viability (Fig. 3 *B*).

A parallel experiment was also carried out for *NSR1* since, in previous experiments showing it to be dispensable, the gene was only partially deleted (Lee et al., 1991). In agreement with the findings of Lee et al. (1991), strains in which the *NSR1* gene was completely deleted were still able to grow, but at a reduced rate. In an attempt to induce a lethal phenotype, the *nsr1::URA3* strain was grown under high stress conditions (osmotic, temperature, or carbon source). Although greatly reduced colony size as compared with the

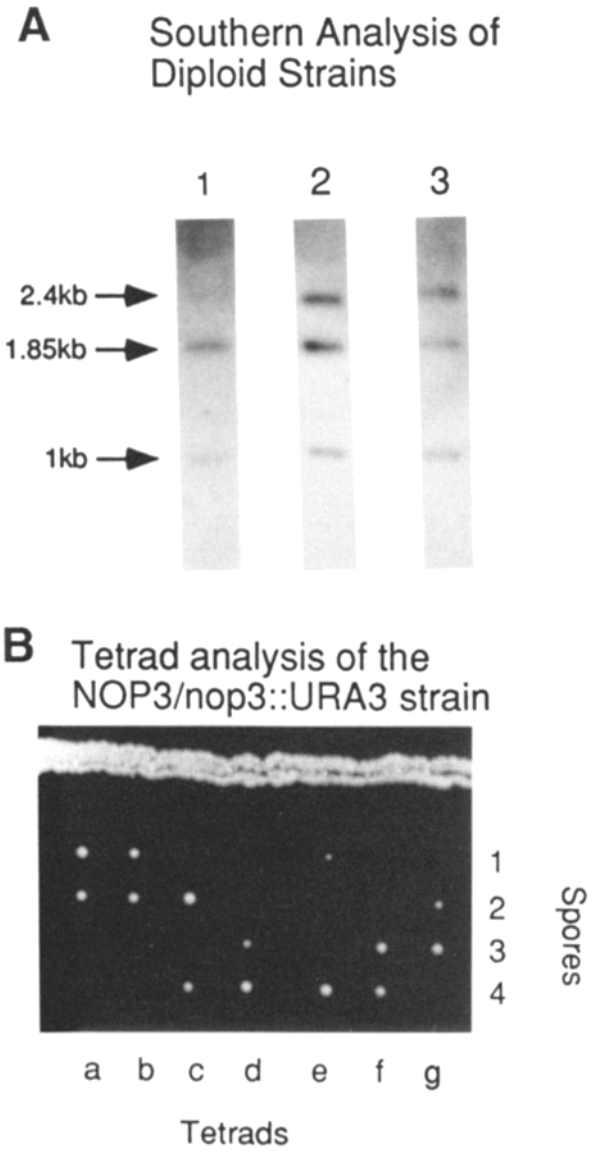

Figure 3. Gene disruption of *NOP3*. (*A*) Southern hybridization of genomic DNA cut with EcoRI and hybridized with a *NOP3* riboprobe. 1.85- and 1-kb EcoRI fragments are detected due to cleavage at an internal EcoRI site within the *NOP3* coding sequence. Lane *1*, DNA extracted from the isogenic homozygous *NOP3* diploid. Lanes *2* and *3*, DNA extracted from two independent *URA3*$^+$ transformants. In each transformant, one copy of the *NOP3* gene has been deleted and replaced with the *URA3*$^+$ selectable marker, resulting in a new 2.4-kb EcoRI fragment. (*B*) *URA*$^+$ transformants were sporulated and tetrads were individually dissected. The figure shows seven tetrads (*a–g*) and the corresponding spores (*1–4*) grown on a YPD plate at 30°C. In each case only two spores from each tetrad were able to form colonies.

NSR1$^+$ control was observed when grown at 18°C and on 20% glycerol, the *nsr1* lesion was not observed to cause lethality.

NOP3 Is Distributed between the Nucleolus and the Nucleoplasm

Antibodies were raised in rabbits against peptide C4, corresponding to the 14 carboxy-terminal amino acid residues of

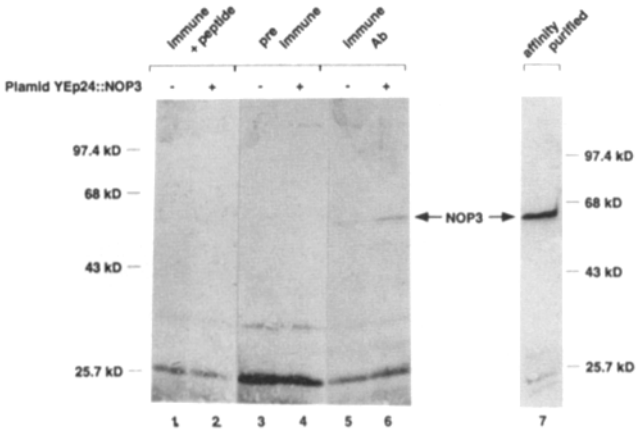

Figure 4. An anti-peptide antibody recognizes a 60-kD band by Western analysis. Western blot of total protein extracts from D150 (lanes *1*, *3*, *5*, and *7*) and an isogenic strain containing YEpNOP3 (lanes *2*, *4*, and *6*). Lanes *1* and *2*, serum raised against peptide C4, preincubated in the presence of the peptide; lanes *3* and *4*, preimmune serum; lanes *5* and *6*, serum raised against peptide C4; lane *7*, antibodies affinity-purified against peptide C4. A specific 60-kD doublet is present in the lanes incubated with the anti-peptide serum or affinity-purified antibodies. Decoration of the 60-kD doublet is specifically blocked when the C4 peptide (1 μg/ml) is present as competitor and is absent from lanes incubated with the preimmune sera.

NOP3. On Western blots of total yeast protein (Fig. 4), the antiserum reacts with a protein with an apparent molecular mass of 60 kD. The signal from this band is increased in a strain carrying the *NOP3* clone on YEp24, a high copy number 2μ plasmid, consistent with overexpression of the NOP3 protein (Fig. 4, lanes *5* and *6*). A slightly smaller species, which may represent a degradation product, is also detected. To demonstrate the specificity of the antibodies, the ability of the C4 peptide to compete with the 60-kD protein for binding of the antibody was tested (Fig. 4, lanes *1* and *2*). Addition of the competitor peptide resulted in the loss of the specific 60-kD band, whereas a nonspecific band with an apparent molecular mass of 25 kD remained unaffected. Other GAR proteins have been previously observed to run anomalously on SDS-PAGE; however, it is not clear whether this is a property of the highly charged GAR domain itself. Anti-NOP3 antibodies were affinity purified from the rabbit serum over a Sepharose column covalently linked to peptide C4. As shown in Fig. 4, lane *7*, the affinity-purified antibodies react strongly only with the 60-kD NOP3 band.

Indirect immunofluorescence with the affinity-purified antibodies against NOP3 (shown in red in Fig. 5) demonstrates that NOP3 is solely localized in the nucleus. In most cases, the antibody decorates the entire nucleus in wild-type cells (Fig. 5 *A*). Nucleolar localization was tested by double labeling with a monoclonal antibody against the nucleolar protein, NOP1 (shown in green in Fig. 5). In most cells, the NOP1 labeling is fully included within the region of NOP3 labeling (Fig. 5 *A*), showing that both the nucleolus and nucleoplasm are decorated by anti-NOP3 antibodies. Neither the nucleoplasmic nor the nucleolar labeling were present if the NOP3 antibodies were first incubated with the competitor peptide (data not shown). In strains lacking functional RNA polymerase I, the nucleolar structure has re-

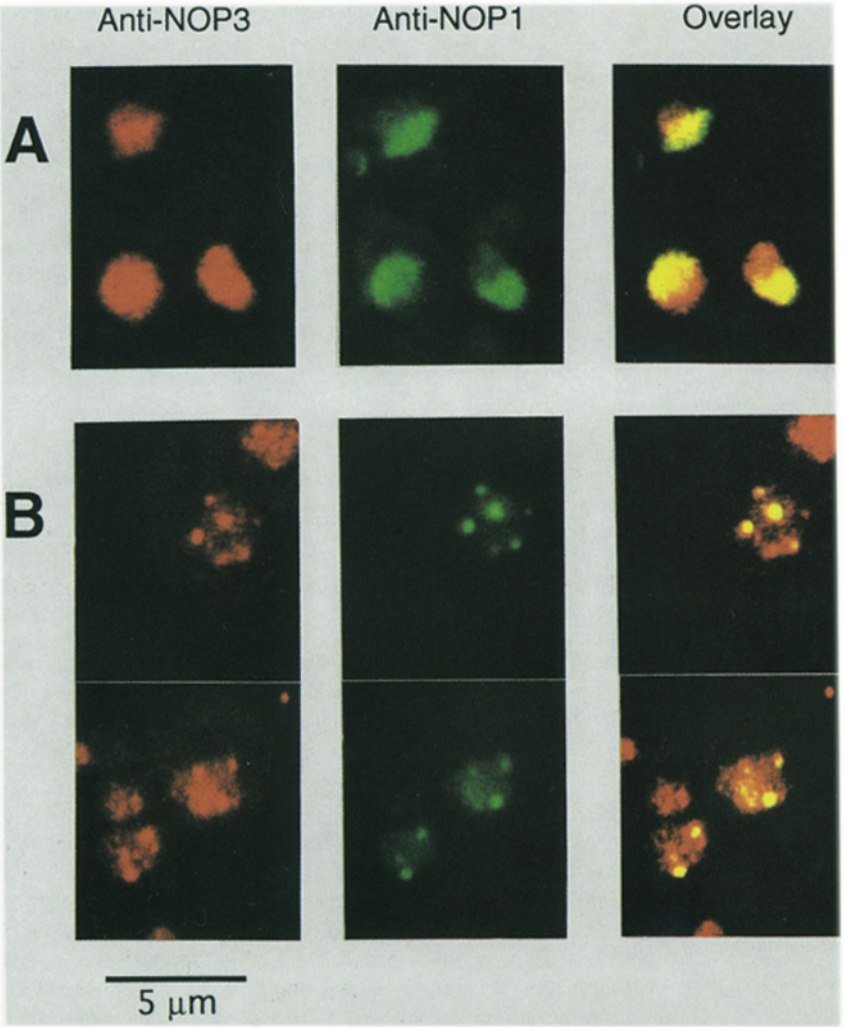

Figure 5. Localization of NOP3 to the nucleus by indirect immunofluorescence. Pseudo-colored confocal images decorated with monoclonal anti-NOP1 antibodies (mAb A66) (*green*) and affinity-purified anti-NOP3 antibodies (*red*). The single images were overlayed and regions of NOP1 and NOP3 colocalization appear as yellow staining. (*A*) Tetraploid yeast strain. (*B*) Strain lacking functional RNA polymerase I, in which pre-rRNA synthesis is driven by an RNA polymerase II *GAL* promoter (strain NOY408-1a; Nogi et al., 1991). In the tetraploid strain, NOP1 shows the classical crescent-shaped staining pattern of yeast nucleolar components, which NOP3 staining also includes the nucleoplasm. In an RNA polymerase I–deficient strain (NOY408-1a), the nucleolus is fragmented and NOP3 becomes more tightly associated with the resulting MNBs, which also contain NOP1. Complexes were detected with FITC-coupled anti–mouse antibodies and Texas Red–coupled anti–rabbit antibodies, respectively.

cently been reported to be disrupted (Oakes, M., Y. Nogi, M. W. Clark, and M. Nomura, manuscript submitted for publication). Fig. 5 *B* shows immunofluorescence of a strain carrying a deletion of the gene encoding the 135-kD subunit of RNA polymerase I whose growth is supported by transcription of the rDNA by RNA polymerase II (Nogi et al., 1991). In this strain NOP1 (shown as green in Fig. 5 *B*) becomes localized to "mini-nucleolar bodies" (MNBs); NOP3 (shown as red in Fig. 5 *B*) is also concentrated in the MNBs in this strain.

Ribosome Synthesis in the GAL::nop3 Strain

To study the effects of NOP3 depletion on ribosome synthesis, a strain was constructed using the regulated *GAL10* promoter to control *NOP3* expression. Using PCR, an 880-bp *NOP3* fragment was subcloned, introducing HindIII/BamHI sites 10 nucleotides upstream from the initiator ATG. A 1.5-kb BamHI/HindIII fragment containing the *URA3* selectable marker and the *GAL10* promoter fused to the *CYC1* nontranscribed leader sequence was isolated from plasmid pLGSD5 (Guarente et al., 1982). This was subcloned into the newly created BamHI/HindIII sites adjacent to the ATG, placing the expression of the *NOP3* gene under the control of the *GAL10* promoter. The *GAL::nop3* construct was introduced into the chromosome of a *ura3*$^-$ haploid strain by transformation on galactose medium with selection for the *URA3*$^+$ marker. In the transformants the *NOP3* promoter should now be separated from the coding sequence by the inserted *URA3-pGAL10-CYC1* fragment. As expected, the haploid transformants grow on galactose but not on glucose media.

For the first 18 h after transfer to glucose minimal medium, the *GAL::nop3* strain has approximately the same doubling time (3 h per generation) as an isogenic wild-type strain. After this time, growth begins to slow (Fig. 6), reaching an estimated 102 h per generation after growth for 50 h in glucose medium. The level of NOP3 was assessed by Western analysis of total protein extracted from the *GAL::nop3* strain during growth in glucose minimal medium using anti-NOP3 antibodies. The level of NOP3 is considerably reduced by 18 h and little is detected after 24 h (data not shown).

The ability of cells depleted of NOP3 for 24 h to produce cytoplasmic ribosomes was investigated by pulse labeling (Fig. 7). Cells were labeled in vivo simultaneously with [^{3}H]uracil and [^{35}S]methionine for 15 and 20 min, respectively. After labeling, the total incorporation of radioactivity in the *GAL::nop3* mutant was 48% of that in the *NOP3*$^+$ strain. Cells were lysed under high salt conditions to dissociate polysomes and 80S ribosomes, and nuclei were pelleted by centrifugation. 40S and 60S ribosomal subunits were separated on a 10–40% sucrose gradient. To directly com-

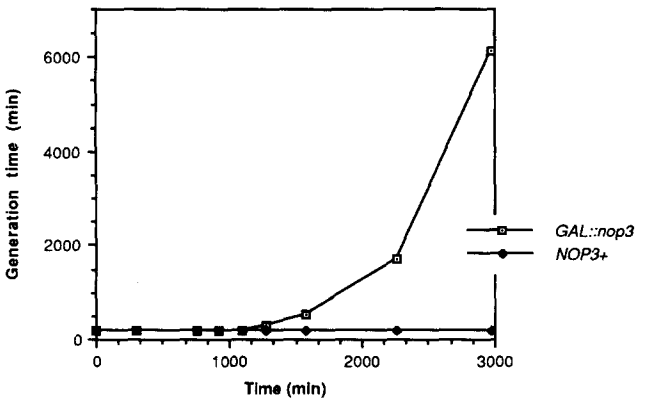

Figure 6. Growth curve of *GAL::nop3* strain after transfer to glucose medium. For the first 18 h in glucose minimal medium, *GAL::nop3* strains grow with the same doubling time (3 h per generation) as the *NOP3*$^+$ strain. Thereafter, growth of the *GAL::nop3*) strain is progressively inhibited. The graph shows the doubling time in minutes per generation against time after transfer to growth in glucose minimal medium.

pare [^{3}H]uracil and [^{35}S]methionine incorporation into ribosomal subunits from the mutant and wild-type strains, equal amounts of incorporated radioactivity were applied to the sucrose gradients for the mutant and wild-type strains. After centrifugation, the gradient was divided into 14 fractions where fraction 1 corresponds to the top of the gradient (Fig. 7) and fraction 14 the bottom. Samples from each fraction were TCA precipitated and the amount of radioactivity incorporated was measured in a scintillation counter.

In the *NOP3*$^+$ strain, the peaks of ^{35}S-labeling (Fig. 7) correspond to the expected mobility of 40S and 60S ribosomal subunits and to the peaks of 18S and 25S rRNA

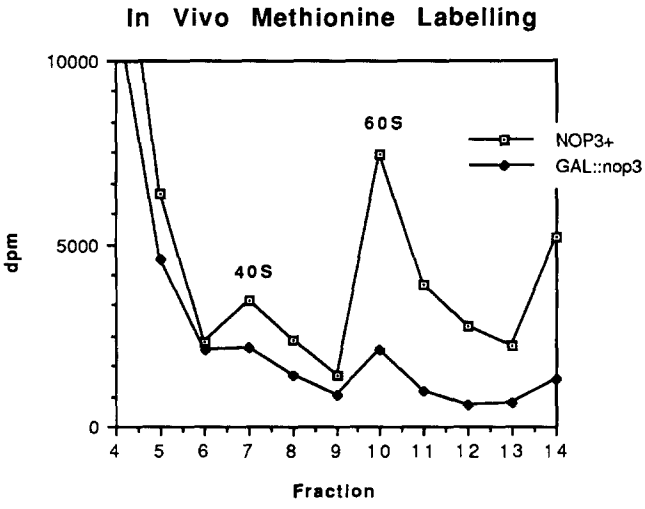

Figure 7. In vivo labeling of 40S and 60S ribosomal subunits. Total cellular protein was pulse-labeled with [^{35}S]methionine for 20 min at 30°C 24 h after transfer of the *NOP3*$^+$ and *GAL::nop3* strain to glucose medium. Cytoplasmic 40S and 60S ribosomal subunits were separated on a 10–40% sucrose gradient, and protein samples from each fraction were TCA precipitated. The incorporation of radioactivity in the *GAL::nop3* strain and a *NOP3*$^+$ strain in each sucrose gradient fraction was measured on a scintillation counter and is represented graphically as a proportion of total protein synthesis.

identified by gel electrophoresis (data not shown). The sucrose gradient mobility of ribosomal subunits extracted from the *GAL::nop3* mutant is identical to those from the *NOP3*$^+$ strain; however, the number of cytoplasmic 40S and 60S ribosomal subunits is greatly reduced in the mutant. Calculation of the area under the graph shown in Fig. 7 indicates that the incorporation into 60S subunits as a proportion of total protein synthesis in the *GAL::nop3* strain is fourfold lower than in the *NOP3*$^+$ strain. The *GAL::nop3* mutant is, therefore, strongly impaired in the synthesis of new cytoplasmic ribosomal subunits after growth for 24 h in glucose medium. The same results were obtained by [^{3}H]uracil labeling of the rRNA (data not shown).

Depletion of NOP3 Affects Pre-rRNA Processing

To determine whether the reduced synthesis of ribosomes in the NOP3-depleted strain is accompanied by aberrant processing of pre-rRNA, steady-state levels of pre-rRNA were analyzed after depletion of NOP3 for 12, 24, 36, and 48 h (Fig. 8). Identical filters were hybridized with probes specific for different pre-rRNA processing intermediates (see Fig. 9 for the locations of the pre-rRNA species and hybridization probes). Within 12 h after transfer to glucose medium, and well before any growth defect is detectable, accumulation of the 35S primary transcript, as well as 27SB and 20S pre-rRNA, is evident (see Fig. 9 *B* for the processing pathway). Even at late time points, when total pre-rRNA transcription is reduced, 27SB strongly accumulates, reaching a peak at 36 h after transfer to glucose medium. At this time, an aberrant 23S pre-rRNA precursor is accumulated, which is probably generated by cleavage of 35S pre-rRNA at or close to site B_1 (see Fig. 9 *A*), liberating 27SB and 23S. The concomitant loss of the 20S pre-rRNA species is observed as 23S accumulates. By 48 h, the major pre-rRNA detected is 27SB. The levels of mature 18S and 25S rRNAs, as visualized by ethidium staining, remain relatively constant until 48 h, when rRNA accumulation falls considerably.

To assess the kinetics of processing, pre-rRNA synthesis was analyzed by pulse-chase labeling of the *GAL::nop3* strain (Fig. 10). After growth for 12, 24, or 36 h in glucose medium, the cells were pulse-labeled at 30°C with [^{3}H-methyl]methionine or [^{3}H]uracil for 2 and 1 min, respectively, and chased with a large excess of unlabeled methionine or uracil for 1, 2.5, and 5.5 min. In contrast to the Northern analysis, no significant differences in pulse–chase labeling were observed after growth for 12 h in glucose medium. 24 h after transfer to glucose medium, processing is greatly slowed, resulting in unprocessed 35S pre-rRNA remaining even after 5.5 min of chase; by comparison, 35S was fully processed by the earliest chase time point in the wild-type strain. Additionally, unprocessed 20S and 27SB pre-rRNAs accumulate, resulting in a reduction in the accumulation of mature 18S and 25S rRNA in the *GAL::nop3* strain. After growth for 36 h in glucose medium, 23S pre-rRNA is detected along with 35S and 27SB pre-rRNA, while the loss of mature 18S and 25S rRNA is complete. The 24- and 36-h labelings of the *GAL::nop3* strain have been exposed ~10-fold longer than the *NOP3*$^+$ and 12-h labelings in Fig. 10. Similar results were obtained by labeling with [^{3}H]uracil (data not shown).

Taken together, the results of the Northern analysis of

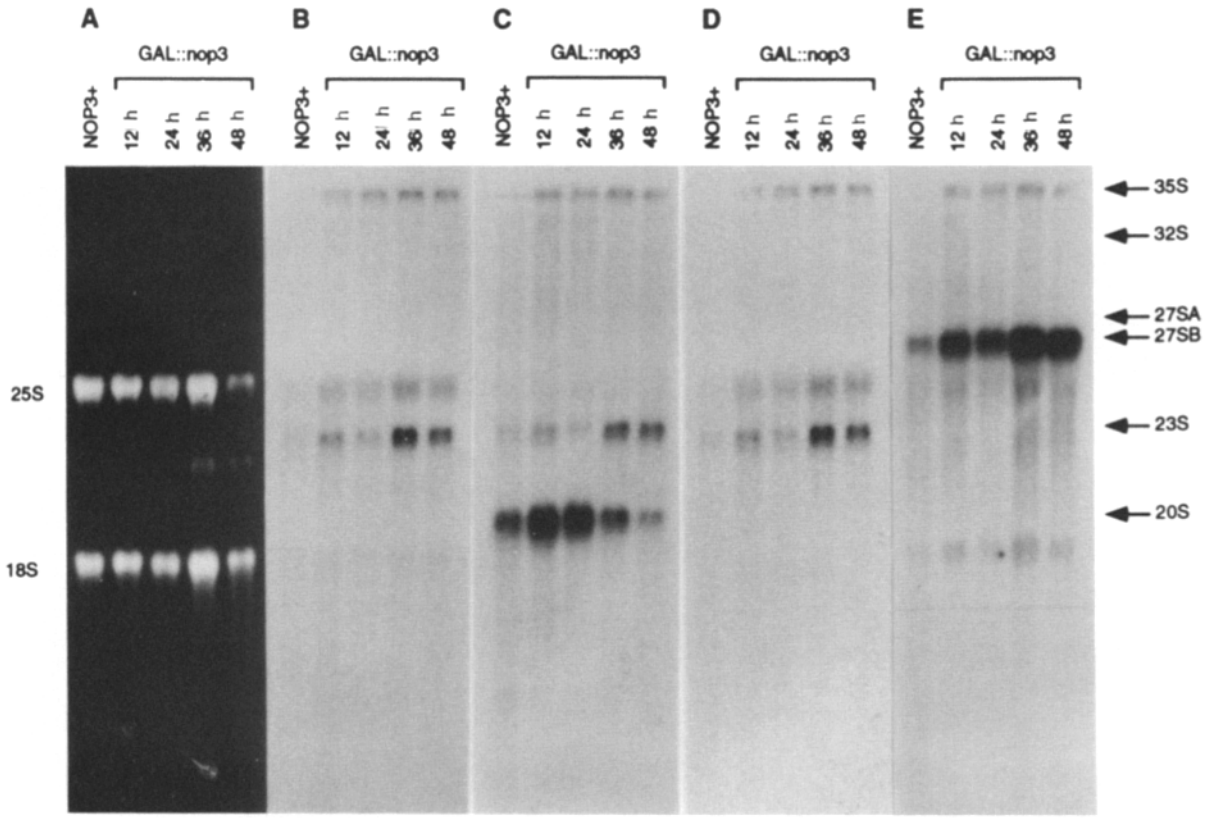

Figure 8. Steady-state levels of rRNA and pre-rRNA in cells depleted of NOP3. Northern analysis of RNA extracted from the *GAL::nop3* strain 12, 24, 36, and 48 h after transfer to glucose medium. As a control, RNA was extracted from the *NOP3*$^+$ strain grown in glucose medium. (*A*) rRNA visualized by staining with ethidium bromide. (*B*) Northern hybridization with oligonucleotide 1, which is specific for a region within the 5′ external transcribed spacer. The oligonucleotide hybridizes to 35S and 23S pre-rRNA. (*C*) Northern hybridization with oligonucleotide 2, which is specific for ITS1 5′ to cleavage site A2. The oligonucleotide hybridizes to 35S, 32S, 23S, and 20S pre-rRNA. (*D*) Northern hybridization with oligonucleotide 3, which is specific for ITS1 3′ to cleavage site A2. The oligonucleotide hybridizes to 35S, 32S, 27SA, and 23S pre-rRNA. (*E*) Northern hybridization with oligonucleotide 4, which is specific for ITS2. The oligonucleotide hybridizes to 35S, 32S, 27SA, and 27SB. The positions of the major pre-rRNA species (35S, 32S, 27SA, 27SB, 23S, and 20S) are indicated by arrows. See Fig. 9 for the positions of the oligonucleotides and for a diagram of the pre-rRNA processing pathway.

steady-state levels of pre-rRNA and the kinetic analysis by pulse–chase labeling show that in the NOP3 depleted strain processing of 35S pre-rRNA is slowed and processing of 27SB pre-rRNA to 25S rRNA and 20S pre-rRNA to 18S rRNA are inhibited. The accumulation of pre-rRNA species observed in Fig. 8 is even more dramatic because, as shown in Fig. 10, transcription of pre-rRNA is clearly reduced, even after 12 h of growth of the *GAL::nop3* strain in glucose medium.

The steady-state levels of snoRNAs and snRNAs were also investigated to confirm that levels remained unchanged during NOP3 depletion and that changes observed in pre-rRNA processing were not due to quantitative changes in snoRNA or snRNA levels. The levels of the snoRNAs U3, U14 (snR128), snR10, and snR190, and the nucleoplasmic snRNAs U4 and U6 remained unchanged during depletion (Fig. 11, *A* and *B*). U5 snRNA levels were observed to fall by ~50% after growth for 36 h in glucose medium. The reason for this is unclear, but this would not be expected to have a direct affect on pre-rRNA processing. The processing of pre-rRNA is impaired in *prp* mutants due to a block in the splicing of pre-mRNAs encoding ribosomal proteins. The splicing of two pre-mRNAs, encoding ribosomal proteins rp29 and S10, was assessed by Northern hybridization during the time course of NOP3 depletion. No alterations in the ratio of pre-mRNA to mRNA were detected (data not shown), making it unlikely that NOP3 plays a role in mRNA splicing.

Discussion

We report here the cloning, sequencing, and functional analysis of a fifth member of the GAR family of proteins in *S. cerevisiae*, which we have named NOP3. The previously identified members of this family are all localized in the nucleolus and are implicated in many aspects of ribosome biogenesis. The approach used also resulted in the cloning of two previously identified GAR proteins, SSB1 and NSR1. Sequence comparisons of the *NOP3* clone with other members of the GAR family reveal a high degree of sequence homology within the GAR domain. However, while previously characterized GAR proteins are localized exclusively in the nucleolus, the in situ labeling of NOP3 encompasses the nucleoplasm as well as the nucleolus. An even nucleoplasmic/nucleolar distribution is observed in the majority of

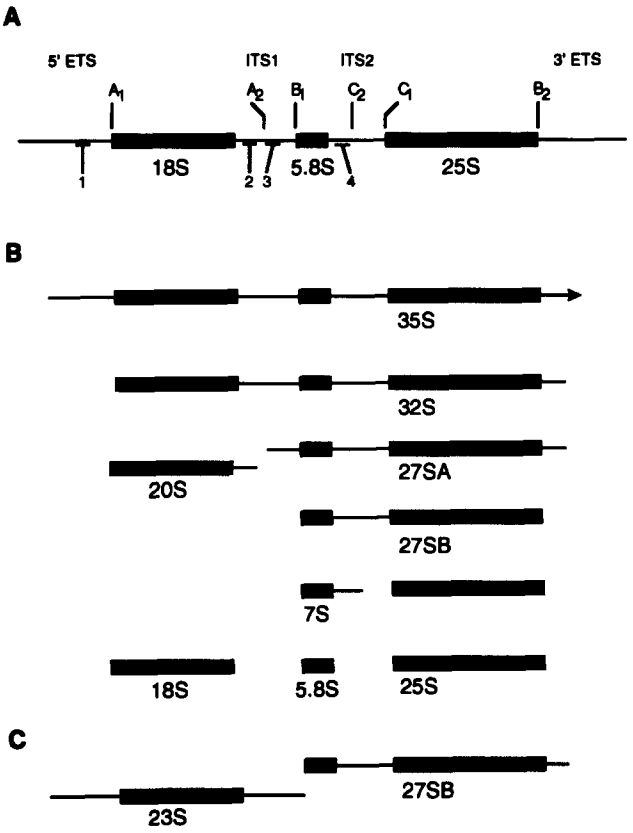

Figure 9. Structure of the *S. cerevisiae* rDNA repeat and processing pathway. (*A*) Structure of the *S. cerevisiae* rDNA repeat indicating the major processing sites and the hybridization probes used for Northern hybridization in Fig. 8. The mature rRNAs are indicated by the boxed areas. (*B*) The major pre-rRNA processing pathway in wild-type yeast cells. (*C*) The probable structure of the 23S/27SB pre-rRNA aberrant processing products resulting from premature cleavage at or near the site B1. The end points of these species have not been determined at the nucleotide level, but Northern hybridization analyses (Fig. 8) show that the 27SB pre-rRNA species does not include the internal transcribed spacer 1 (ITS1), while 23S pre-rRNA extends beyond site A2 and includes sequences from the 5′ external transcribed spacer.

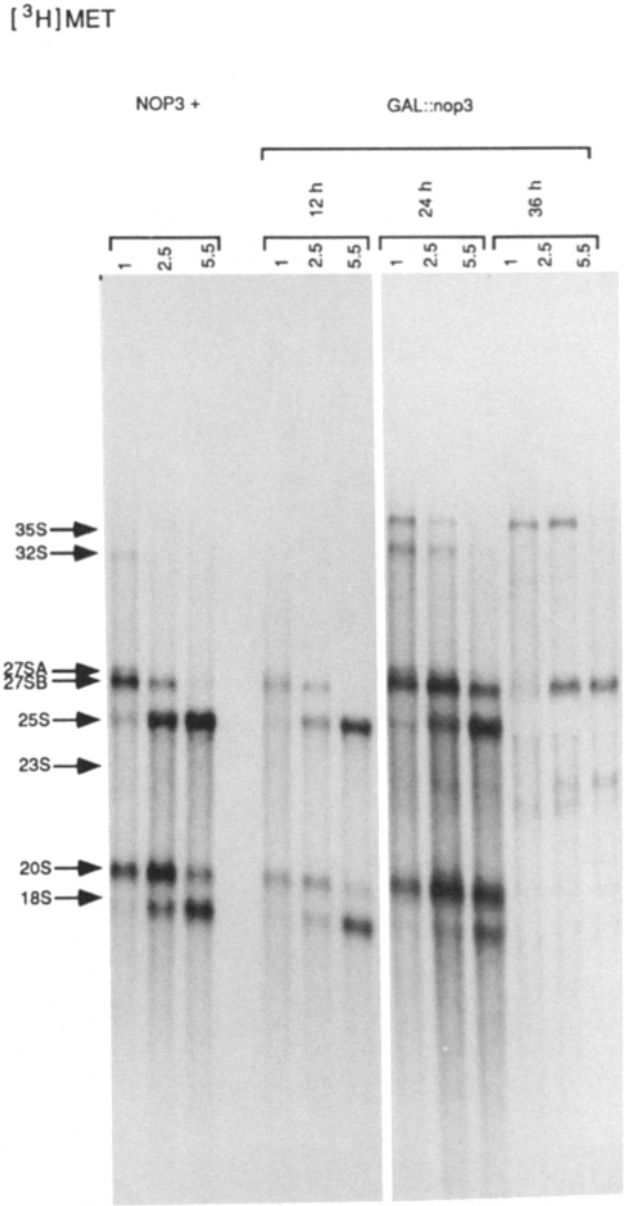

Figure 10. Pulse–chase analysis of pre-rRNA from the *NOP3*$^+$ and *GAL::nop3* strains during the time course of NOP3 depletion. Cells were pulse-labeled for 2 min at 30°C with [^{3}H-methyl]methionine and chased with excess unlabeled methionine for 1, 2.5, or 5.5 min as indicated. The RNA was extracted and separated on an agarose/formaldehyde gel, transferred to Genescreen+ membrane and labeled bands visualized by fluorography. The positions of the major pre-rRNAs are indicated by the arrows. The fluorographs of RNA extracted from the *GAL::nop3* strain grown for 24 and 36 h on glucose medium have been exposed 10-fold longer than those from the *NOP3*$^+$ and *GAL::nop3* strain grown for 12 h on glucose medium.

cells, although predominantly nucleoplasmic or nucleolar staining is observed in a very small minority. In yeast strains lacking functional RNA polymerase I the nucleolus breaks down and nucleolar components become localized to structures described as mini-nucleolar bodies (MNBs) (Oakes, M., Y. Nogi, M. W. Clark, and M. Nomura, manuscript submitted for publication). SSB1, NOP1, and NOP3 all become enriched in the MNBs, indicating an association between NOP3 and the nucleolar components.

To determine whether the lethality of *nop3*$^-$ cells is due to defective ribosome synthesis, we placed *NOP3* under the control of the regulated *GAL10* promoter, allowing the expression of *NOP3* to be specifically inhibited by glucose media. In vivo pulse labeling of the newly synthesized proteins and RNA, and hence 40S and 60S ribosomal subunits, after 24 h growth in glucose medium, indicates that the synthesis of ribosomal subunits as a proportion of total protein synthesis in the *GAL::nop3* mutant is 25% of that in a *NOP3*$^+$ strain.

Inhibition of pre-rRNA processing is detected by Northern analysis as early as 12 h after transfer to glucose medium even though the growth rate of the *GAL::nop3* strain does not fall until 18 h after transfer. In pulse–chase labeling experiments performed 24 h after transfer to glucose medium, inhibition of the processing of 27SB pre-rRNA to 25S rRNA and 20S pre-rRNA to 18S rRNA is clearly observed. The processing of 35S pre-rRNA, which is normally extremely

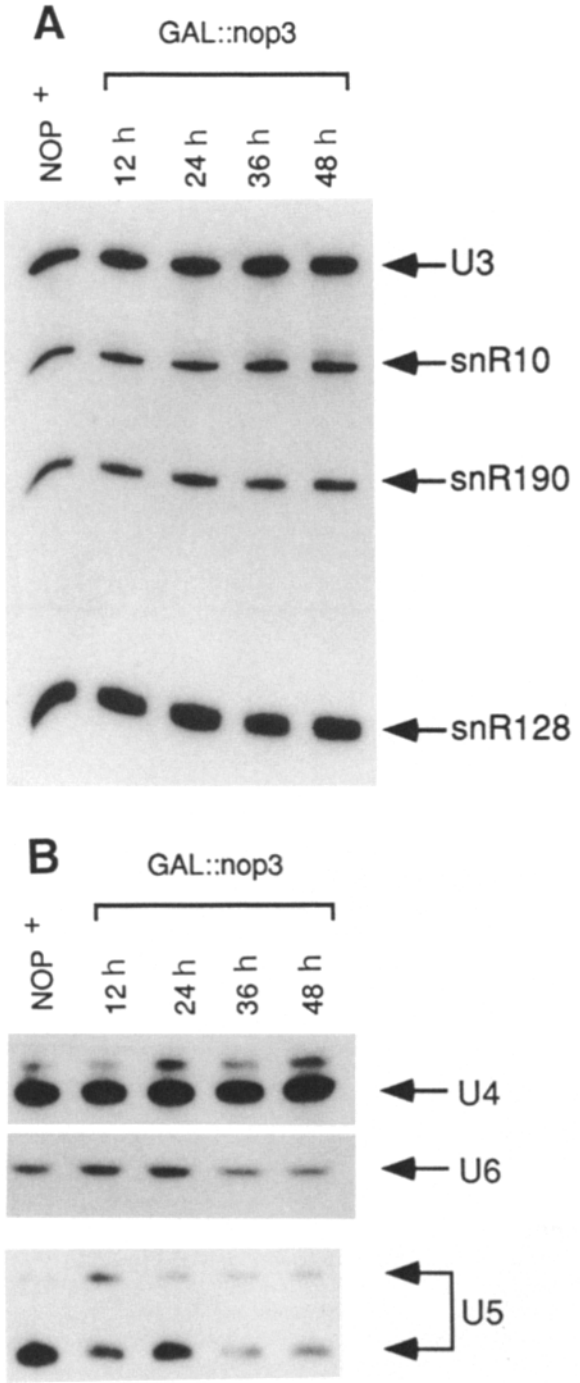

Figure 11. Steady-state levels of snoRNAs and snRNAs in cells depleted of NOP3. Northern analysis of RNA extracted from the *NOP3*$^+$ and *GAL::nop3* strains. The same preparations of RNA as in Fig. 8 were used. The levels of snoRNAs U3, snR10, snR190, and snR128 are shown in *A*. The levels of the snRNAs U4, U5, and U6 are shown in *B*.

rapid in wild-type yeast, is also slowed, resulting in its accumulation.

In strains carrying mutations in the snoRNAs, U3, U14, snR10, or snR30, or in the snoRNA-associated proteins NOP1 or GAR1, an alternative pre-rRNA processing pathway is detected in which the 5′ region of the pre-rRNA is processed to a 23S species normally seen only at very low levels in wild-type yeast strains (Tollervey, 1987; Li et al., 1990; Hughes and Ares, 1991; Tollervey et al., 1991; Girard et al., 1992; Morrissey, J. P., and D. Tollervey, manuscript submitted for publication). This arises from cleavage of the 35S primary transcript at or near site B_1 without prior cleavages at A_1 and A_2 (see Fig. 9) producing 27SB pre-rRNA in conjunction with the aberrant 23S species. For all except mutations in snR10, the 23S pre-rRNA is likely to be very rapidly degraded, preventing synthesis of 18S rRNA. In the *GAL::nop3* strain, the majority of 35S pre-rRNA is processed through this alternative pathway only late in the time course of depletion, after growth for 36 h or more in glucose medium, suggesting that this may be a secondary effect of NOP3 depletion.

Pre-rRNA processing defects have also been documented for mutants implicated in preribosomal particle assembly. Temperature-sensitive mutations in L16 (Moritz et al., 1990), a ribosomal protein normally assembled as part of the 60S ribosomal subunit, prevent the maturation of 27SB pre-rRNA to 25S rRNA. This strain is still able to process 20S pre-rRNA to 18S rRNA and can assemble functional 40S subunits (Moritz et al., 1991). Similarly, in *rrp1* and *spb4* mutants, which are also likely to be defective in ribosome assembly, processing is again blocked between 27S pre-rRNA and 25S rRNA (Fabian and Hopper, 1987; Sachs and Davis, 1990). Taken together, these results suggest that assembly of the pre-rRNA with r proteins is an essential prerequisite for the late cleavage events. This may function as a "proof-reading" mechanism, ensuring that ribosomal subunits are correctly assembled before the final cleavages to produce the mature rRNAs and finally functional ribosomes.

Depletion of NOP3 clearly has a dramatic effect on pre-rRNA processing and ribosome synthesis, but we do not know whether NOP3 acts directly or indirectly in pre-rRNA processing. One conceivable role, consistent with the internuclear distribution of NOP3, would be a function involved in the transport of proteins destined for the nucleolus between the nucleoplasm and the nucleolus. Active nucleoplasmic/nucleolar transport has not previously been described, although the protein Nopp140 has been proposed to play some role in the transport of ribosomal components (Meier and Blobel, 1992). Passive diffusion of the necessary components from the nucleoplasm to the nucleolus may not be able to support the high levels of ribosome biogenesis in yeast, and may be difficult to reconcile with the low reported pool size of free ribosomal proteins in yeast (see Warner, 1982). The entire ribosomal contents of the cell must be synthesized within ~90 min, corresponding to ~40 ribosomes/s. This represents a requirement for ~2,000 ribosomal proteins/s to be imported or 10 ribosomal proteins/s per nuclear pore complex. There may be a requirement for a system to move ribosomal proteins from the inside of the nuclear pore complex to the nucleolus. NOP3 is a potential candidate for a nucleoplasmic/nucleolar transport component, perhaps fulfilling a role as a nucleolar import receptor.

We would like to thank M. Nomura and M. Oakes for providing the RNA polymerase I deleted strain (NOY 408-1a) and for communicating results before publication, J. Aris for providing the monoclonal antibody against NOP1 (mAb A66), M. Carmo-Fonseca for assistance with immunofluorescence and confocal microscopy, Hanna Lehtonen for expert technical assistance, and Yves Henry, Iain Mattaj, John Morrissey, and Heather Wood for critical reading of the manuscript. During the course of this work P.

Silver and colleagues also identified NOP3, and we thank them for communicating their results before publication.

Received for publication 26 May 1992 and in revised form 10 June 1992.

References

Clark, M. W., M. L. R. Yip, J. Campbell, and J. Abelson. 1990. SSB-1 of the yeast *Saccharomyces cerevisiae* is a nucleolar-specific, silver-binding protein that is associated with the snR10 and snR11 small nucleolar RNAs. *J. Cell Biol.* 111:1741–1751.

Dandekar, T., and D. Tollervey. 1989. Cloning of *Schizosaccharomyces pombe* genes encoding the U1, U2, U3 and U4 snRNAs. *Gene (Amst.).* 81:227–235.

Fabian, G. R., and A. K. Hopper. 1987. RRP1, a *Saccharomyces cerevisiae* gene affecting rRNA processing and production of mature ribosomal subunits. *J. Bacteriol.* 169:1571–1578.

Ghisolfi, L., G. Joseph, F. Amalric, and M. Erard. 1992. The glycine-rich domain of nucleolin has an unusual supersecondary structure responsible for its RNA-helix-destabilizing properties. *J. Biol. Chem.* 267:2955–2959.

Girard, J. R., H. Lehtonen, M. Caizergues-Ferrer, F. Amalric, D. Tollervey, and B. Lapeyre. 1992. GAR1 is an essential nucleolar RNP protein required for pre-rRNA processing in yeast. *EMBO (Eur. Mol. Biol. Organ.) J.* 11:673–682.

Guarente, L., R. R. Yocum, and P. Gifford. 1982. A *GAL10-CYC1* hybrid yeast promoter identifies the *GAL4* regulatory region as an upstream site. *Proc. Natl. Acad. Sci. USA.* 79:7410–7414.

Henríquez, R., G. Blobel, and J. P. Aris. 1990. Isolation and sequencing of NOP1. *J. Biol. Chem.* 265:2209–2215.

Hernandez-Verdun, D. 1991. The nucleolus today. *J. Cell Sci.* 99:465–471.

Hughes, J. M. X., and M. Ares. 1991. Depletion of U3 small nucleolar RNA inhibits cleavage in the 5′ external transcribed spacer of yeast pre-ribosomal RNA and impairs formation of 18S ribosomal RNA. *EMBO (Eur. Mol. Biol. Organ.) J.* 10:4231–4239.

Ito, H., Y. Fukuda, K. Murata, and A. Kimura. 1983. Transformation of intact yeast cells treated with alkali cations. *J. Bacteriol.* 153:163–168.

Jong, A. Y. S., M. W. Clark, M. Gilbert, A. Oehm, and J. L. Campbell. 1987. *Saccharomyces cerevisiae* SSB1 protein and its relationship to nucleolar RNA-binding proteins. *Mol. Cell Biol.* 7:2947–2955.

Kenan, D. J., C. C. Query, and J. D. Keene. 1991. RNA recognition: towards identifying determinants of specificity. *TIBS (Trends Biochem. Sci.).* 16: 214–220.

Lapeyre, B., H. Bourbon, and F. Amalric. 1987. Nucleolin, the major nucleolar protein of growing eucaryotic cells: an unusual protein structure revealed by nucleotide sequence. *Proc. Natl. Acad. Sci. USA.* 84:1472–1476.

Lee, W. C., Z. Xue, and T. Mélèse. 1991. The *NSR1* gene encodes a protein that specifically binds nuclear localization sequences and has two RNA recognition motifs. *J. Cell Biol.* 113:1–12.

Li, H. V., J. Zagorski, and M. J. Fournier. 1990. Depletion of U14 small nuclear RNA (snR128) disrupts production of 18S rRNA in *Saccharomyces cerevisiae*. *Mol. Cell Biol.* 10:1145–1152.

Maniatis, T., E. T. Fritsch, and J. Sambrook. 1989. Molecular Cloning: A Laboratory Manual. 1.94–1.104. Cold Spring Harbor Laboratory, Cold Spring Harbor, NY.

Meier, U. T., and G. Blobel. 1992. Nopp140 shuttles on tracks between nucleolus and cytoplasm. *Cell.* 70:127–138.

Moritz, M., A. G. Paulovich, Y.-F. Tsay, and J. L. Woolford. 1990. Depletion of yeast ribosomal proteins L16 or rp59 disrupts ribosome assembly. *J. Cell Biol.* 111:2261–2274.

Moritz, M., B. A. Pulaski, and J. L. Woolford. 1991. Assembly of 60S ribosomal subunits is perturbed in temperature sensitive yeast mutants defective in ribosomal protein L16. *Mol. Cell Biol.* 11:5681–5692.

Nogi, Y., R. Yano, and M. Nomura. 1991. Synthesis of large rRNAs by RNA polymerase II in mutants of *Saccharomyces cerevisiae* defective in RNA polymerase I. *Proc. Natl. Acad. Sci. USA.* 88:3962–3966.

Ochs, R. L., M. A. Lischwe, W. H. Spohn, and H. Busch. 1985. Fibrillarin: a new protein of the nucleolus identified by autoimmune sera. *Biol. Chem.* 54:123–134.

Sachs, A. B., and R. W. Davis. 1990. Translation initiation and ribosomal biogenesis: involvement of a putative rRNA helicase and RPL46. *Science (Wash. DC).* 24:1077–1079.

Schimmang, T., D. Tollervey, H. Kern, R. Frank, and E. C. Hurt. 1989. A yeast nucleolar protein related to mammalian fibrillarin is associated with small nucleolar RNA and is essential for viability. *EMBO (Eur. Mol. Biol. Organ.) J.* 8:4015–4024.

Tollervey, D. 1987. A yeast small nuclear RNA is required for normal processing of pre-ribosomal RNA. *EMBO (Eur. Mol. Biol. Organ.) J.* 6:4169–4175.

Tollervey, D., H. Lehtonen, M. Carmo-Fonseca, and E. C. Hurt. 1991. The small nucleolar RNP protein NOP1 (fibrillarin) is required for pre-rRNA processing in yeast. *EMBO (Eur. Mol. Biol. Organ.) J.* 10:573–583.

Tyc, K., and J. A. Steitz. 1989. U3, U8 and U13 comprise a new class of mammalian snRNPs localized in the cell nucleolus. *EMBO (Eur. Mol. Biol. Organ.) J.* 8:3113–3119.

Warner, J. R. 1982. The yeast ribosome: structure, function and synthesis. *In* The Molecular Biology of the Yeast Saccharomyces. Vol. II. J. N. Strathern, E. W. Jones, and J. R. Broach, editors. Cold Spring Harbor Laboratory Press, Cold Spring Harbor, NY. 529–560.

Zagorski, J. D., D. Tollervey, and M. J. Fournier. 1988. Characterization of an SNR gene locus in Saccharomyces cerevisiae that specifies both dispensible and essential snRNAs. *Mol. Cell. Biol.* 8:3282–3290.